Biogeosciences Discuss., 10, 4539–4574, 2013
www.biogeosciences-discuss.net/10/4539/2013/
doi:10.5194/bgd-10-4539-2013

Biogeosciences
Discussions
Open Access

Seasonal dynamics of methane emissions from a subarctic fen in the Hudson Bay Lowlands

K. L. Hanis[1], M. Tenuta[1], B. D. Amiro[1], and T. N. Papakyriakou[2]

[1]Dept. Soil Science, University of Manitoba, Winnipeg, Manitoba, Canada
[2]Dept. Environment and Geography, University of Manitoba, Winnipeg, Manitoba, Canada

Received: 15 February 2013 – Accepted: 23 February 2013 – Published: 8 March 2013

Correspondence to: M. Tenuta (mario.tenuta@ad.umanitoba.ca)

Published by Copernicus Publications on behalf of the European Geosciences Union.

Abstract

Ecosystem-scale methane (CH_4) flux (F_{CH_4}) over a subarctic fen at Churchill, Manitoba, Canada was measured to understand the magnitude of emissions during spring and fall shoulder seasons, and the growing season in relation to physical and biological conditions. F_{CH_4} was measured using eddy covariance with a closed-path analyzer in four years (2008–2011). Cumulative measured annual F_{CH_4} (shoulder plus growing seasons) ranged from 3.0 to 9.6 g CH_4 m^{-2} yr^{-1} among the four study years, with a mean of 6.5 to 7.1 g CH_4 m^{-2} yr^{-1} depending upon gap-filling method. Soil temperatures to depths of 50 cm and air temperature were highly correlated with F_{CH_4}, with near surface soil temperature at 5 cm most correlated across spring, fall, and the whole season. The response of F_{CH_4} to soil temperature at the 5 cm depth and air temperature was more than double in spring to that of fall. Emission episodes were generally not observed during spring thaw. Growing season emissions also depended upon soil and air temperatures but water table also exerted influence with F_{CH_4} highest when water was 2–13 cm below and least when it was at or above the mean peat surface.

1 Introduction

Organic soils (peatlands) have the highest mean soil organic carbon contents of any permafrost-affected soil in the northern circumpolar permafrost region with global inventories of 94 to 184 Pg carbon in the top 3 m (Tarnocai et al., 2009). Terrestrial regions of the Arctic, including peatlands, are estimated to have sequestered between 300 and 600 Tg C yr^{-1} since 1975 (McGuire et al., 2009). However, the radiative forcing benefit of a carbon dioxide (CO_2) sink is partially offset by the emission of 30 to 100 Tg yr^{-1} methane (CH_4) for the terrestrial arctic (McGuire et al., 2009), of which 2.3 Tg CH_4 yr^{-1} are emitted from the Hudson Bay Lowlands in Canada (Pickett-Heaps et al., 2011). This is important because CH_4 has a radiative forcing of about 33 times

BGD
10, 4539–4574, 2013

Seasonal dynamics of methane emissions from a subarctic fen

K. L. Hanis et al.

that of CO_2 over 100 yr when including the direct and indirect radiative effects of aerosol responses (Shindell et al., 2009), 25 times that of CO_2 directly (Forster et al., 2007).

Previous studies of CH_4 fluxes (F_{CH_4}) in northern peatlands have focussed on the period of peak productivity of vegetation (mid-summer) (e.g. Verville et al., 1998; Updegraff et al., 2001; Grondahl et al., 2008) and examined the effects of water table height (e.g. Turetsky et al., 2008; Long et al., 2009; Zona et al., 2009), temperature (e.g. Verville et al., 1998; Wille et al., 2008; Long et al., 2009), and plant communities, in particular, hydrophytes with aerenchyma tissues for plant-mediated transport of rhizosphere gases to the atmosphere (e.g. Schimel, 1995; Long et al., 2009) on emissions. Consequently, an understanding of growing season F_{CH_4} and associated drivers is being developed; however, more research is needed to understand fluxes outside of the main growing season. Little is known about F_{CH_4}during the shoulder periods of spring-melt and fall freeze-up. These periods may be important to understand the conditions driving the transition in emission to and from should periods and the growing season.

Recent attention has focused on CH_4 emission bursts during the spring and fall seasons from northern peatlands. Tokida et al. (2007) described episodic release of CH_4 from bubbles in ice overlying an ombrotrophic bog in Japan during spring-melt, and Hargreaves et al. (2001) reported spring-melt F_{CH_4} bursts from a Finnish minerotrophic flark fen dominated by graminoids. Fall freeze-up F_{CH_4} bursts have also been reported to occur during freeze-thaw cycles in the same Finnish flark fen (Hargreaves et al., 2001) and in a graminoid fen in Greenland underlain by permafrost (Mastepanov et al., 2008).

Emission bursts could contribute substantially to annual F_{CH_4}, but they are ephemeral and spatially variable, and the drivers are still not clearly understood. More research is needed at northern circumpolar peatlands during the shoulder seasons of spring-melt and fall freeze-up to focus on understanding the trends and magnitude of F_{CH_4} and the associated drivers of emissions over different spatial and temporal scales.

BGD
10, 4539–4574, 2013

The objectives of this study were to determine ecosystem scale F_{CH_4} from an eutrophic subarctic fen to understand (a) the magnitude of emissions during spring-melt and fall-freeze-up periods relative to the growing season, and (b) the environmental conditions contributing to emissions. We hypothesized that F_{CH_4} is a well-behaved function of temperature given favourable water table conditions in peatlands. We tested this through campaign measurements of whole-ecosystem F_{CH_4} using an eddy-covariance flux tower during spring and fall campaigns and for four growing seasons from 2008 to 2011.

2 Methods

2.1 Site description

The study site is a eutrophic palsa fen (fen) (NWWG, 1997) near Churchill, Manitoba, Canada (58°39′57′ N, 93°49′48″ W). It is situated within the boreal forest-tundra ecotone, which is a transitional zone extending approximately 10 km inland from the Hudson Bay coastline, and within the zone of continuous permafrost (Brown, 1970). The fen hosts three dominant landscape units: hummocks, sedge-lawns, and hollows. The hummocks and sedge-lawns have 30 to 40 cm of peat over carbonate-rich glaciomarine sediments (Rouse et al., 2002). The active layer can extend to more than 1.5 m in depth.

The sedge-lawn landscape unit is the most extensive, covering approximately 55 % of the fen (Raddatz et al., 2009) and is dominated by the sedge *Carex aquatilis* Wahlenb., as well as other *Carex* spp., the grasses *Eriophorum* spp., *Calamagrostis* spp., and *Arctagrostis latifolia* (R. Br.) Griseb., rushes *Juncus* spp., horsetail *Equisetum variegatum* Schleich. ex F. Weber & D. Mohr, and an understory of the moss, *Pseudocalliergon turgescens* (Jensen) Loeske. The sedge-lawn landscape unit is at the mean water-table, peat-surface interface at an elevation of 16.56 ± 0.4 m (S.D., $n = 29$ sample points) with the *P. turgescens* being submersed during periods of a high water table

BGD
10, 4539–4574, 2013

(often June, September and October), and exposed during periods of a low water table (often July and August). *C. aquatilis* is the principal vascular plant at the fen and can facilitate CH_4 transport to the atmosphere (Schimel, 1995). New shoots emerge from mid- to late June; flowering occurs in mid-July and senescence begins in late August.

The vegetation of hummocks is dominated by the lichens *Cladina stellaris* (Opiz) Brodo and *Cladonia rangiferina* (L.) Nyl., the moss *Dicranum elongatum* Schwaegr., as well as heath vegetation *Betula glandulosa* Michx., *Salix arctophila* Cock. ex Heller, *Rhododendron tomentosum* Harmaja, *Andromeda polifolia* L., *Rhododendron lapponicum* (L.) Wahlenb., *Vaccinium vitis-idaea* L. ssp. *minus* (Lodd.) Hultén, and *V. uliginosum* L. The hummocks are drier mounds that rise above the level of the sedge-peat surface by about 40 cm. The hollows were about 55 cm below the sedge-peat surface with mats of *P. turgescens*, and partially decomposed peat material at their base, overlying a mineral substrate. They typically were filled with water, except during extreme drought periods.

The water table for the fen fluctuates throughout the growing season, with a typical annual variation of 15 cm below to 20 cm above the mean sedge-peat elevation. The maximum water table height usually occurs just after spring snow-melt as the result of the top-down melting of the fen, with water overlying ice at the peat surface. Snow-melt occurred from 23–26 May (day of year (DOY) 144–147) 2008, 11–13 June (DOY 162–164) 2009, 9–14 May (DOY 129–134) 2010 and 30 May–4 June (DOY 150–155) 2011. The fen was snow and ice covered by 26, 13 and 30 of October (DOY 300, 286, 303) in 2008, 2009 and 2010 respectively, but ice covered on 23 October (DOY 296) and snow covered on 7 November (DOY 311) 2011.

2.2 Eddy covariance flux station

An eddy covariance flux station was established in June of 2008 to measure F_{CH_4} and Net Ecosystem Exchange (NEE). The station was off-grid, powered by wind (Model 200 Whisper Wind Generator, Southwest Windpower Inc., Flagstaff, AZ), solar (five

BGD
10, 4539–4574, 2013

photovoltaic panels for 500 W combined), and gas power generation (EU2000i, Honda Inc. as supplemental).

The CH_4 concentration of atmosphere was measured using a closed-path analyzer (RMT-200 Fast Methane Analyzer (Los Gatos Research Inc., Mountain View, CA) (Baer et al., 2002; Hendriks et al., 2008; Baldocchi et al., 2011)). The RMT-200 measurement range was 0.1 to 25 ppmv with < 1 % uncertainty (Los Gatos Research, 2009). Methane concentrations were sampled at 10 Hz and the pressure in the cavity was maintained at 19 kPa. Air was drawn from 4.27 m above the fen surface to the analyzer through a mesh screen (Cole Parmer, Vernon Hills, IL) and 7 µm inline filter (Swagelok, Solon, OH), and 18 m of PTFE-Teflon tubing (6.35 mm i.d.; Zeus Inc., Orangeburg, SC). An XDS 35i dry vacuum scroll pump (Edwards, Crawley, West Sussex, UK) drew the air stream at a flow rate of 28.5 L min^{-1} during the 2008 field season with a sample lag of 1.2 s. In 2009, this scroll pump failed and was replaced with two diaphragm vacuum pumps connected in parallel (LABOPORT N840.3, KNF Neuberger, Inc., Trenton, NJ) at a combined flow of 4.6 L min^{-1} and a calculated lag of 7.5 s. This replacement of the high-flow pump with a more reliable lower-flow pump was also done by Detto et al. (2011) at their site. For us, the lower power draw was an added advantage of the slower pumps.

A 3-dimensional ultrasonic anemometer-thermometer (CSAT3, Campbell Scientific Inc., Logan, UT) was center-mounted at the same height as the gas sample inlet facing north to measure wind velocities and air temperature. Additionally, an open-path CO_2/H_2O analyzer (LI-7500, LI-COR Biosci., Lincoln, NE), center-mounted at a 35° angle facing north at the same height of the gas sample inlet and wind anemometer, was used to determine CO_2 and water vapour molar densities. Data were recorded at 10 Hz by a CR3000 datalogger (Campbell Scientific Inc.).

Wind velocities, CO_2 and H_2O densities were recorded nearly continuously. However, due to power generation and storage constraints, the CH_4 analyzer and pumps could only operate for campaign periods of 2 to 24 h before the battery storage bank was depleted for the 2008, 2009 and 2010 field seasons. In order to compensate for the

BGD
10, 4539–4574, 2013

power limitations and still capture diurnal trends in F_{CH_4} during the 2011 field season, a relay turned the pumps on for 37 min to capture a 30 min campaign (5-min prior to and 2-min after the half hour) starting at 00:00, 03:00, 09:00, 11:00, 15:00, 16:00, 17:00 and 21:00 LT. We recognize that there are gaps in our flux measurements where an ephemeral release could have been missed.

2.3 Supporting environmental variables

Air temperature (T_{air}) was measured at a height of 1.8 m (HMP45C, Vaisala Inc., Woburn, MA), horizontal wind speed (u) and direction at 4 m (Model 05103, R.M. Young Co., Traverse City, MI), photosynthetically active radiation (PAR) at 1 m (PAR Lite sensor, Kipp & Zonen, Bohemia, NY), and rainfall at 0.5 m (TR-525M, Texas Electronics Inc., Dallas, TX). Soil temperature was measured using thermocouples in two wood dowels at 10, 20, 30, 40, 50, and 60 cm depths, placed in a sedge-lawn (T_{sed10}, T_{sed20}, T_{sed30}, T_{sed40}, T_{sed50}, and T_{sed60}) and a hollow (T_{hol10}, T_{hol20}, T_{hol30}, T_{hol40}, T_{hol50}, and T_{hol60}). Three-junction averaging thermocouples were also placed at 5 cm depth in three hummocks, sedge-lawns and hollows to provide an average near-surface temperature (T_{soil5}). Environmental variables were recorded half hourly using dataloggers (CR5000, CR1000, CR23X, Campbell Scientific Inc.). Water table height was read daily from stationary rulers in three hollows during all four field seasons, and recorded half hourly by three pressure transducers (HOBO U20 Water Level Data Loggers, Onset Computer Corporation, Inc., Pocasset, MA) in the 2011 field season. Elevation of ruler tops and the sedge-peat surface (29 locations) were determined by GPS (TSC1 Asset Surveyor, Trimble Navigation Ltd., Sunnyvale, CA).

2.4 Data analysis

Half-hourly eddy coveriance fluxes were calculated using MATLAB (R2007a, The Math Works Inc., Natick, MA) user-defined functions. Spikes in the measured high-frequency data were removed based on thresholds for each signal set to identify single spurious

BGD
10, 4539–4574, 2013

values. Block-average covariances were calculated without detrending and then coordinate rotated for each 30-min period (Tanner and Thurtell, 1969). The covariances were maximized half-hourly by adjusting lag delays. High-frequency losses of the closed-path CH_4 analyzer were calculated by comparing the fractional loss of energy in the F_{CH_4} spectrum to the spectrum for sensible heat flux. This resulted in a correction of 1.5 % for the high-volume pump in 2008 and 12 % for the low-volume pump in the other years. Density effects were corrected for water vapour for the closed-path CH_4 system, and for both heat and water vapour for the open-path CO_2 system (Webb et al., 1980). Self-heating of the LI-7500 analyzer was included based on the corrections of Burba et al. (2008).

F_{CH_4} data from the CH_4 analyzer were filtered to omit values when only one of the two diaphragm pumps was running, the mirror ring-down value had declined more than 20 %, or when the internal pressure < 18 kPa. NEE data were filtered when rain and particles intercepted the sensor path based on the analyzer's diagnostic report. All F_{CH_4} determinations were filtered to remove half-hour periods at night (PAR < 10 µmol $m^{-2}\,s^{-1}$) when the friction velocity (u^*) was below a threshold of 0.2 m s^{-1} ($u^*_{threshold}$). NEE data were restricted to midday values from 11:00 to 15:00 local time (NEE_{MD}) when plant productivity would be highest. F_{CH_4} and NEE_{MD} data were filtered to remove half-hourly periods when the cardinal wind direction was 135–225° to exclude directions from the tower and gas power generator. Upward fluxes are defined as positive.

To observe seasonal trends and determine environmental drivers of F_{CH_4} during the spring, fall and growing seasons. The data was divided into specific periods: spring of 2009 (DOY 150–190, 2009), all springs (DOY 150–190, 2008–2011), fall of 2011 (DOY 260–320, 2011), all falls (DOY 260–320, 2008–2011), and all shoulder + growing seasons (DOY 150–320, 2008–2011).

Pearson's product-moment correlation analysis was performed on all half-hourly F_{CH_4} data and T_{air}, T_{soil5}, T_{sed10}, T_{sed20}, T_{sed50}, T_{hol10}, T_{hol20}, T_{hol50}, NEE_{MD}, water table and PAR with $P < 0.0001$ set as significant. Correlations were done to show relationships

BGD
10, 4539–4574, 2013

for spring of 2009, all springs, fall of 2011, all falls, and all shoulder + growing seasons. The strength of the Pearson's product-moment correlation was graded on a scale: strong correlation when $R \geq \pm 0.80$, moderate correlation when $\pm 0.79 \geq R \geq \pm 0.50$, and weak correlation when $R \leq \pm 0.49$.

Temperature-response of F_{CH_4} was determined using linear regression analysis for 1 °C bin-averaged 30-min F_{CH_4} data for all springs, all falls and all shoulder + growing seasons using both T_{air} and T_{soil5}. Water-table-response of F_{CH_4} was determined using linear regression analysis for 1-cm-height bin-averaged 30-min F_{CH_4} for the same time periods. The strength of the linear relationship between F_{CH_4} and environmental variables was graded on a scale: strong linear relationship when $r^2 \geq \pm 0.80$, moderate relationship when $\pm 0.79 \geq r^2 \geq \pm 0.50$, and weak relationship when $r^2 \leq \pm 0.49$. The slope of the response of F_{CH_4} to a change in temperature (ΔF_{CH_4} °C^{-1}) or water table (ΔF_{CH_4} m^{-1}) was done using the Student's-t statistic calculated as the difference between slopes divided by the standard error of the difference between slopes at $n-4$ degrees of freedom (Kleinbaum and Kupper, 1978) using SigmaPlot 11.0 (Systat Software, Inc., San Jose, CA).

Mean daily F_{CH_4} values were reported from the average of 30-min emissions without gap-filling missing periods in a day. Cumulative annual methane emissions were estimated by summing the mean daily fluxes for all days when daily mean air temperature ≥ 0 °C by (1) using linear interpolation to gap-fill missing days between measured $F_{CH_4}(\Sigma F_{CH_4-GF_1})$, (2) using linear interpolation to fill 30-min gaps between measured $F_{CH4}(\Sigma F_{CH_4-GF_2})$, and (3) modelling the missing 30-min F_{CH_4} values using the T_{soil5} linear regression relationship with F_{CH_4} (for all shoulder + growing seasons) up to 12 °C ($\Sigma F_{CH_4-GF_3}$). Above this temperature, the flux was assumed constant at 47 nmol CH_4 m^{-2} s^{-1} based on our measurements.

BGD
10, 4539–4574, 2013

3 Results

3.1 Weather conditions

Monthly mean T_{air} and total precipitation for the 2008 field season showed that it was warmer than normal for all study months, drier than normal for July and November and wetter than normal in August (Table 1). Seasonally from May to November, T_{air} was 1.4 °C warmer, and had 67.9 mm less precipitation than the long-term average.

In 2009 cooler and wetter than normal conditions were experienced early in the season from May to July, followed by warmer and drier conditions in the fall from September to November. Seasonal totals indicate that T_{air} was 0.6 °C cooler and had 47.9 mm less precipitation than the long-term average for May to November.

In 2010, conditions were warmer and wetter than normal for July and August, with precipitation in August being 265 % greater than normal. Fall conditions from September to November were warmer and drier than normal. Seasonally from May to November, T_{air} was 1.6 °C warmer, and had 51.1 mm more precipitation than the long-term average.

2011 conditions showed that it was warmer than normal in July and throughout the fall from September to November. Drier than normal conditions occurred in September and November, while wetter than normal conditions occurred in October. Seasonal totals indicate that T_{air} was 2.1 °C warmer and had 9.9 mm more precipitation than the long-term average for May to November.

3.2 Spring F_{CH_4}

We were able to monitor the spring melt of 2009 (Fig. 1). In other years only the post-melt period was captured. The spring of 2009 was categorized into three periods: the snow and ice-covered Pre-Melt (DOY 150 to 161), the transitional Melt period from snow and ice cover to open water (DOY 162 to 173), and Post-Melt (DOY 174 to 190) when no ice was present above the peat to inhibit F_{CH_4} diffusion.

BGD
10, 4539–4574, 2013

During the 2009 Pre-Melt period, F_{CH_4} was near zero (−6 to 8 nmol CH_4 m^{-2} s^{-1}). T_{air} was mostly below 0 °C until DOY 158, and temperatures at all soil depths were less than 0 °C. Midday net CO_2 flux (NEE_{MD}) ranged from 0 to 2 µmol CO_2 m^{-2} s^{-1}.

Throughout the 2009 Melt period, T_{air} was mostly above 0 °C, with daytime highs between 5 and 15 °C. Soil temperatures were less than 0 °C until DOY 168 when T_{soil5} > 0 °C but the deeper soil remained frozen. By DOY 167, most of the fen surface thawed and was free of ice and snow and the water table dropped from 22 cm above the peat surface to < 1 cm below the surface by DOY 172. During the Melt period F_{CH_4} increased from near zero to 20 nmol CH_4 m^{-2} s^{-1} and NEE_{MD} ranged from 1 to 3 µmol CO_2 m^{-2} s^{-1}.

In the 2009 Post-Melt period, F_{CH_4} gradually increased to have midday peaks of 40 to 110 nmol CH_4 m^{-2} s^{-1} by DOY 188. A diurnal pattern in F_{CH_4} was evident that followed T_{air} and T_{soil5}. Air temperature remained above 0 °C throughout the period and daytime highs gradually increased from 10 to 23 °C; T_{soil5} reached daytime highs of 14 °C by the end of the period. The 10-cm soil depth thawed on DOY 177 and other soil depths remained frozen. The water table gradually lowered to 8 cm below the peat surface by DOY 188 and NEE_{MD} emissions ranged from 1 to 3 µmol CO_2 m^{-2} s^{-1}.

F_{CH_4} during the 2009 Post-Melt period was similar to F_{CH_4} across all springs (Fig. 2); mean daily F_{CH_4} ranged from 30 to 70 nmol CH_4 m^{-2} s^{-1}. Across all springs T_{soil5} increased from −1 to 17 °C, with T_{soil5} for spring of 2009 being within range but lowest of all springs. NEE_{MD} was dominated by respiration (0 to 3 µmol CO_2 m^{-2} s^{-1}) until DOY 180 across all springs. After DOY 180, uptake of CO_2 by the plants began to outweigh respiration; with the general trend across all springs showing NEE_{MD} transition from 2 to −2 µmol CO_2 m^{-2} s^{-1} by DOY 190 except for the spring of 2009 which remained respiration-dominated until after DOY 190. Early season water table was variable due to the timing of melt ranging from 2 to 12 cm below the peat surface across all springs. The levels in 2009 were within this range.

BGD
10, 4539–4574, 2013

3.3 Fall F_{CH_4}

The fall of 2011 provided the most extensive coverage of F_{CH_4} (Fig. 3). This was divided into two periods: Pre-Freeze with senesced vegetation and mean daily $T_{air} > 0\,^\circ C$ (DOY 260 to 289), and Freeze-Up when ice formed over standing water at the fen and mean daily T_{air} and soil temperatures were $\leq 0\,^\circ C$ by the end of the period (DOY 290 to 320).

During the Pre-Freeze period F_{CH_4} ranged from 55 to 0 nmol $CH_4\,m^{-2}\,s^{-1}$, T_{air} ranged from 20 to $-1\,^\circ C$ and T_{soil5} was between 12 and $2\,^\circ C$. F_{CH_4} gradually declined over the period following the decreasing temperature trend. The water table was 5 to 10 cm below the peat surface until DOY 286 then increased to 6 cm above the surface by the end of the period. NEE_{MD} ranged from 2 to -3 µmol $CO_2\,m^{-2}\,s^{-1}$.

Freeze-Up period surface ice cover developed quickly with a $10\,^\circ C$ drop in T_{air} (from 3 to $-7\,^\circ C$) over 3 days (DOY 290–293) then melted and froze again on DOY 294. The soil temperature profile reversed on DOY 290, after which the surface remained colder than lower depths until convergence to $0\,^\circ C$ by DOY 317. By the end of the period, both T_{air} and T_{soil5} were at or below $0\,^\circ C$. NEE_{MD} emissions ranged from 0 to 1 µmol $CO_2\,m^{-2}\,s^{-1}$ and the final water table measurement of the season on DOY 294 was 1 cm above the peat surface. Freeze-Up F_{CH_4} was minimal (< 6 nmol $CH_4\,m^{-2}\,s^{-1}$ emission) for most of the period, however emission bursts were observed on three occasions. Our visitation of the research site resulted in breaking through surface ice and a F_{CH_4} emission burst on DOY 294 at 17:00 (161 nmol $CH_4\,m^{-2}\,s^{-1}$ over 30-min period). Two non-disturbance related emission bursts were observed over 30-min periods on DOY 298 at 17:30 where F_{CH_4} was 20 nmol $CH_4\,m^{-2}\,s^{-1}$ and on DOY 302 at 11:30 where F_{CH_4} was 34 nmol $CH_4\,m^{-2}\,s^{-1}$. In both instances of non-disturbance related emission bursts, wind speed was low ($\leq 1.4\,m\,s^{-1}$) for two hours leading up to and during the episodes. T_{air} had been below $0\,^\circ C$ for 3.5 days then went above $0\,^\circ C$ for 5.5 h prior to the emission burst on DOY 298, while T_{air} had been below $0\,^\circ C$ for 4 h and then went above $0\,^\circ C$ for 3 h before

BGD
10, 4539–4574, 2013

Seasonal dynamics of methane emissions from a subarctic fen

K. L. Hanis et al.

the emission burst on DOY 302. T_{soil5} was at or above 0 °C before and during both naturally-occurring emission burst events.

F_{CH_4} gradually decreased across all falls with mean daily F_{CH_4} declining from 30 to 5 nmol CH_4 m^{-2} s^{-1} prior to freeze and from 5 to −1 nmol CH_4 m^{-2} s^{-1} during freeze-up (Fig. 2). Fluxes during the fall of 2011 were within the range of those across all falls. T_{soil5} gradually declined from 10 to −1 °C with T_{soil5} being coolest in 2008 and warmest in 2011. NEE_{MD} became primarily emission again of 0 to 2 µmol CO_2 m^{-2} s^{-1} over all falls as *C. aquatilis* senesced and soil respiration outweighed photosynthetic uptake of the plants, however there was still some CO_2 uptake during the fall of 2011 from DOY 260–270. NEE_{MD} emissions across all falls minimized to near zero during freeze-up. From DOY 260 to 290 across all falls, the water table was 1 to 10 cm below the mean peat surface; then increased precipitation prior to freeze-up raised the water table to 2 to 6 cm above the mean peat surface. In the fall of 2011, water table was lower than other years from DOY 260–280, and was higher than other years from DOY 289–292.

3.4 Growing season F_{CH_4}

F_{CH_4} peaked between DOY 190 and 230 with emissions ranging between 30 and 130 nmol CH_4 m^{-2} s^{-1} in 2008, 2009 and 2011 (Fig. 2). This peak in emissions occurred during maximum T_{soil5} (5 to 17 °C), flowering of *C. aquatilis*, peak CO_2 uptake (0 to −6 µmol CO_2 m^{-2} s^{-1}) by the ecosystem, and water table residing 2 to 15 cm below the peat surface (Fig. 2).

Growing season F_{CH_4} measurements in 2010 were very different than other growing seasons. In 2010, F_{CH_4} was minimal between DOY 190 and 200, with emissions of 10 to 25 nmol CH_4 m^{-2} s^{-1} compared to other years where the range was 30 to 90 nmol CH_4 m^{-2} s^{-1} (Fig. 2 and Fig. 4). During the same time period in 2010, T_{soil5} ranged from 13 to 17 °C and NEE_{MD} uptake ranged from near 0 to −5 µmol CO_2 m^{-2} s^{-1}. Water table was 5 to 6 cm below the peat surface, and total rainfall was 8 mm (Figs. 2 and 4). The

BGD
10, 4539–4574, 2013

month prior to these measurements was warmer and drier than normal with a mean monthly T_{air} of 1.1 °C above the 1971–2000 climate normal, and total monthly precipitation of 32 mm below the normal (Table 1). The 2010 growing season F_{CH_4} then peaked between 35 and 65 nmol CH_4 m^{-2} s^{-1} for DOY 200 to 210 with increasing T_{soil5} and a re-wetting of the soil to create warm anaerobic conditions (Fig. 2 and Fig. 4). However, F_{CH_4} rapidly declined again to < 12 nmol CH_4 m^{-2} s^{-1} between DOY 220 and 230, coinciding with a dramatic cooling trend of T_{soil5} from 23 to 8 °C. Emissions continued to be suppressed from DOY 230 to 240 with a rapid rise in water table resulting from several multi-day rain events. A large rainfall event (110 mm in 24 h) on DOY 236 raised the water table 12 cm above the peat surface (Fig. 4). Coincidentally, F_{CH_4} began to increase as the water table dropped, immediately following this event.

3.5 Cumulative annual CH_4 emissions

Cumulative annual CH_4 emissions varied by study year and with gap-filling method (Table 3). The 2008 study year had the highest cumulative annual CH_4 emissions ranging from 6.6 to 9.6 g CH_4 m^{-2} yr^{-1} while the 2010 study year had the lowest cumulative annual CH_4 emissions ranging from 3.0 to 7.2 g CH_4 m^{-2} yr^{-1}. Despite the range in cumulative annual CH_4 emissions estimated by the three gap-filling methods on a yearly basis, the means among the three methods were within 9 % of each other when averaged over all four study years (mean ±1SE = 6.5 ± 0.6 to 7.1 ± 1.1 g CH_4 m^{-2} yr^{-1}).

3.6 Association of F_{CH_4} and environmental variables

Pearson's product-moment correlation analysis proved temperature to be the strongest driver of F_{CH_4} during spring of 2009 and across all springs (Table 2). In spring of 2009, T_{air} and soil temperatures to a depth of 50 cm showed moderate to strong positive correlation ($0.68 \leq R \leq 0.89$), water table had a moderate negative correlation with F_{CH_4} ($R = -0.66$) indicating that as the water table dropped F_{CH_4} increased and NEE_{MD} had a moderate positive correlation with F_{CH_4} ($R = 0.53$). Across all springs, T_{air} and soil

BGD
10, 4539–4574, 2013

Seasonal dynamics of methane emissions from a subarctic fen

K. L. Hanis et al.

temperatures to a depth of 50 cm also showed moderate to strong positive correlation ($0.72 \leq R \leq 0.85$), and water table also showed moderate negative correlation ($R = -0.70$) when compared to spring of 2009. All other variables were not significantly correlated with F_{CH_4} across all springs.

The strongest driver of F_{CH_4} during fall of 2011 and across all falls was soil temperature at 5 cm depth. In fall of 2011, F_{CH_4} had a moderate positive correlation with T_{soil5} ($R = 0.75$) as well as with T_{air} and all other soil temperatures ($0.63 \leq R \leq 0.74$) and PAR ($R = 0.55$). All other variables were not significantly correlated with F_{CH_4} for fall of 2011. Across all falls, F_{CH_4} had a strong positive correlation with T_{soil5} ($R = 0.86$) and with T_{hol10}, T_{hol20}, T_{hol50}, T_{sed10} and T_{sed20} ($R = 0.8$). T_{air}, T_{sed50}, NEE_{MD} and PAR had moderate positive correlations with F_{CH_4} ($0.57 \leq R \leq 0.77$) across all falls, while all other variables were not significantly correlated with F_{CH_4}.

Over all shoulder + growing seasons, T_{air}, T_{soil5} and T_{sed10} had moderate positive correlations ($0.52 \leq R \leq 0.57$) with F_{CH_4}. Other soil temperatures, water table and PAR had weak correlations with F_{CH_4} and NEE_{MD} was not a statistically significant driver of F_{CH_4}.

F_{CH_4} had a strong, positive linear relationship with T_{soil5}, from 0 to 15 °C, for all springs ($r^2 = 0.94$), and from 0 to 12 °C for all falls ($r^2 = 0.89$) and over all shoulder + growing seasons ($r^2 = 0.95$) (Fig. 5). The slope of the linear regression across all springs was more than triple that across all falls and the slopes were significantly different ($P < 0.001$). Positive linear relationships with T_{air} (from 0 to 30 °C) were strong across all springs ($r^2 = 0.91$) and across all shoulder + growing seasons ($r^2 = 0.91$) and moderate across all falls ($r^2 = 0.63$). The slope of the regression across all springs was 4.5 times greater than across all falls and the slopes were significantly different ($P < 0.001$).

F_{CH_4} had a negative linear relationship with water table from 13 cm below to 3 cm above the peat surface with the strongest relationship for all springs ($r^2 = 0.89$). A moderate linear relationship occurred across all shoulder + growing seasons ($r^2 = 0.52$), but there was no linear relationship across all falls ($r^2 = 0.03$). The slope of the

BGD
10, 4539–4574, 2013

regression across all springs was significantly different ($P < 0.001$) than the slope of the regression for all falls. Over the four study years, the highest F_{CH_4} occurred when the water table was 2 to 15 cm below the mean peat surface. It was least when the water table was at or above the mean peat surface.

4 Discussion

4.1 F_{CH_4} response to spring-melt and fall freeze-up

A gradual increase in F_{CH_4} with increasing T_{air} and near-surface soil temperature (T_{soil5} and T_{sed10}) and lowering of the water table was observed across all springs, whereas a gradual decline in F_{CH_4} across all falls occurred with decreasing T_{air}, soil temperature and rising water table. We did not observe a F_{CH_4} burst in spring of 2009 or across all springs. However, we believe to have successfully captured two naturally-occurring 30-min emission bursts of 20 to 34 nmol CH_4 m^{-2} s^{-1} (compared to background emissions of < 6 nmol CH_4 m^{-2} s^{-1}) during fall of 2011 despite our non-continuous measurements.

These naturally-occurring emission bursts in the fall of 2011 happened during periods of low wind speed (< 1.4 m s^{-1}) when air temperature that was below 0 °C formed a thin ice layer over the standing water at the fen, then went above 0 °C for several hours causing the ice to melt. Surface soil temperatures were at or above 0 °C indicating that methane could still be produced and captured as bubbles under the ice, being released as the ice melted. A human-induced 30-min emission burst of 161 nmol CH_4 m^{-2} s^{-1} measured after breaking through thin ice in the fall of 2011 showed that physical disturbance released trapped gas bubbles to the atmosphere analogously to naturally-occurring melt of the ice. However since this disturbance was not only to the ice but to the underlying peat as well, a larger emission burst was observed than naturally-occurring bursts at our fen.

BGD
10, 4539–4574, 2013

We have also observed bubbles within winter ice at the fen and ice of shallow lakes in the area, which have been reported by Duguay et al. (2002). These winter-trapped bubbles did not cause abrupt fluxes from our fen in the spring. It is hypothesized that these gases were gradually released by diffusive processes through the ice over the winter period, and therefore were not released from the bubbles as emission bursts during spring melt. We did not measure F_{CH_4} over the winter period, and given the negligible fluxes from frozen surfaces, it is likely that winter is not a large contributor to annual fluxes despite the potential for bubbles. Further, the gases released from these bubbles during melt contributed to the overall spatial average flux measured with the flux tower, and they were not special events when we consider the seasonal pattern over a large area. We recognize that there are gaps in our flux measurements where an ephemeral CH_4 emission burst could have been missed during spring melt or fall freeze-up.

Other groups have observed CH_4 release during spring melt in northern peatlands due to bubbles trapped in and under ice. Continuous spring melt F_{CH_4} measurements, using eddy covariance with a tunable diode laser over a mesotrophic flark fen in Finland showed peak emission of 75 nmol CH_4 m^{-2} s^{-1} over a six-hour period compared to a range of 12 to 50 nmol CH_4 m^{-2} s^{-1} for the other times (Hargreaves et al., 2001). However, unlike our fen, no permafrost was present at the Finnish fen and soil was thawed from the surface to 40 cm depth. Wille et al. (2008) also used the eddy covariance with a tunable diode laser to determine F_{CH_4} for wet low-centered polygonal tundra in the Lena River Delta, Siberia in pre- and post-melt periods. During melt, F_{CH_4} was highly variable with multiple emission bursts with 1 to 4 h sustained peaks ranging from 87 to 104 nmol CH_4 m^{-2} s^{-1} and then fluxes stabilized between −34 and 34 nmol CH_4 m^{-2} s^{-1} after the melt. The region was within the zone of continuous permafrost, and polygon centers were thawed > 20 cm with standing water during the emission burst events. Tokida et al. (2007) used chambers to measure spring-melt emissions for an ombrotrophic peatland in Japan and found an emission burst as high as 439 nmol CH_4 m^{-2} s^{-1} over a one-hour period. Their ombrotrophic peatland was not

BGD
10, 4539–4574, 2013

underlain by permafrost, and air temperatures throughout the winter and spring-melt period hovered around 0 °C resulting in diurnal freeze-thaw cycles and soil waterlogged conditions. Mastepanov et al. (2008) reported similar results as observed in our study for a graminoid fen underlain by continuous permafrost at Zackenberg Valley, north-east Greenland. Measurements were made with automated chambers and a closed-path CH_4 analyzer. No emission bursts were observed during spring-melt, rather CH_4 emissions were small, but gradually increased to 35 nmol CH_4 m^{-2} s^{-1} by mid-summer. They did observe several emission bursts during freeze-up of 2008 of up to 313 nmol CH_4 m^{-2} s^{-1}.

It is suspected that sites without permafrost that have winters where the average T_{air} is warmer than 0 °C are more likely to be ones where F_{CH_4} emission bursts occur in the spring. Milder winter temperatures will be more conducive to shallow frozen soil layers, methane accumulation over winter, as well as a more rapid surface thaw in spring facilitating emission bursts. This has been shown at the Finnish aapa mire (Hargreaves et al., 2001) that had a mean winter temperature of 0.4 °C and at the ombrotrophic peatland in Japan (Tokida et al., 2007) that had a mean winter temperature of 7 °C, both of which lacked permafrost. In contrast, it is suspected that for sites with permafrost and winters that have an average T_{air} colder than 0 °C there is a greater likelihood that the spring melt F_{CH_4} will be gradual. Cold winter temperatures will impede methane production over winter, soil will be frozen to depths greater than 1 m, and surface thaw will be slower. This was observed at our fen which had a mean winter temperature of −7 °C and at the graminoid fen at Zackenberg Valley, Greenland (Mastepanov et al., 2008) that had a mean winter temperature of −9 °C, both of which had continuous permafrost.

4.2 Controls of F_{CH_4}

In the current study, F_{CH_4} was strongly associated with T_{air} and all soil temperatures up to a depth of 50 cm during all springs, all falls, and all shoulder + growing seasons. The temperature response was significantly greater across all springs than across

BGD
10, 4539–4574, 2013

all falls. Soil temperatures to a depth of 10 cm were found to be the most effective drivers of F_{CH_4} at our fen. Similarly to our site, other eddy covariance studies from northern peatlands have reported soil temperatures from surface to 50 cm depth to be related to F_{CH_4}. Rinne et al. (2007) found F_{CH_4} related best to T_{soil} at 35 cm depth at the boreal minerotrophic fen, Siikaneva, Finland, for March 2005–February 2006. They also showed the relationship was also well suited to the spring of 2005. Long et al. (2009) reported that for a moderately rich treed fen during the frost-free season near Athabaska, Alberta, Canada, T_{soil} at 50 cm depth had the best relationship with F_{CH_4}. Permafrost was not present at either of these sites. In contrast, Hargreaves et al. (2001) reported the surface temperature (0–10 cm) of their aapa mire complex with no permafrost present to be best related to F_{CH_4} for 15–28 August 1995 and 29 September–18 October 1998, incorporating the freeze-up period. The subarctic palsa mire, Stordalen, Sweden, which is underlain by discontinuous permafrost, studied by Jackowicz-Korzynski et al. (2010) from 4 May–16 December 2006 and 3 May–31 December 2007 showed the best relationship with T_{soil} at 3 cm depth. Wille et al. (2008) found that T_{soil} at 20 cm depth was best related to F_{CH_4} from wet polygon centres underlain by continuous permafrost in the central Lena River Delta, Siberia for 18 July–24 October 2003 and 4 June–22 July 2004. Tagesson et al. (2012) reported surface soil temperature of 2 cm depth to be best related to F_{CH_4} for a patterned fen underlain by continuous permafrost at Zackenberg, Greenland over two consecutive growing seasons: 24 June–16 September 2008 and 1 June–6 September 2009. Most studies have reported a single F_{CH_4}–soil temperature relationship during the growing season, and very few have reported on spring melt or fall freeze up period F_{CH_4} relationships. Our data indicate increased understanding of drivers when spring and fall relationships of F_{CH_4} with T_{air} and soil temperature profiles to 50 cm depth are evaluated separately.

For our palsa fen underlain by continuous permafrost, the near-surface active layer is the source of production leading to spring and fall F_{CH_4} rather than release of trapped CH_4 deeper in the soil. The greater response in F_{CH_4} to T_{soil5} during the spring than fall may be related to the gradual release of labile carbon from plant roots, residues and

BGD
10, 4539–4574, 2013

microbial biomass broken down over winter and early spring freeze-thaw cycles as the soil profile thaws. Edwards et al. (2006) measured microbial biomass and available soil carbon, nitrogen and phosphorus from late winter (T_{soil} from 5 to 15 cm depth below −10 °C), through 49 days of freeze-thaw cycles (1 April–19 May), and early spring (T_{soil} from 5 to 15 cm above 0 °C) of 2005 at a nearby wet sedge meadow dominated by *Carex aquatilis* at Churchill, Manitoba. Results from their study indicated that microbial biomass and nutrient availability peaked during the freeze-thaw cycles and steadily declined in early spring. At our fen, the thick ice layer resulting from a high water table in fall insulated the soil and prolonged the thaw at 5-cm depth until mid-June and the 20-cm depth until mid-July. It is suspected that the peak in microbial biomass and available carbon are spread over the same time frame.

Water table position was correlated to F_{CH_4} at our fen during spring of 2009, across all springs and across all shoulder + growing seasons. The highest F_{CH_4} occurred when the water table was between 2 and 13 cm below the mean peat surface with soil temperatures from surface to 20 cm depth ≥5 °C. However, there appears to be a wide range of controlling water table depths that are site dependent. For example, Zona et al. (2009) found the highest F_{CH_4} when the water table was at the peat surface and soil temperature at 10 cm ≥ 4 °C at a wet, sedge meadow tundra, underlain by continuous permafrost at Barrow, Alaska. Turetsky et al. (2008) used clear static chambers and showed the highest F_{CH_4} when the water table was 0 to 10 cm below the peat surface and soil temperature at 25 cm ≥ 14 °C at a moderately rich fen near Fairbanks Alaska in the zone of discontinuous permafrost. Hendriks et al. (2010) used dark static chambers at a eutrophic peat meadow, not underlain by permafrost, at Horstermeer, Netherlands, and found the highest F_{CH_4} with surface soil temperature ≥ 10 °C and a water table 20 to 40 cm below the peat surface. This range indicates that understanding where CH_4 is being produced in the peat profile and the transport mechanisms under varying water table positions is important.

F_{CH_4} was less when the water table rose above the mean sedge-peat surface of our fen. Zona et al. (2009) observed similar results for a wet sedge meadow tundra near

BGD
10, 4539–4574, 2013

Barrow, Alaska. In our study, a large late summer rain (110 mm in 24 h in 2010) raised the water table 12 cm above the peat surface. F_{CH_4} subsequently increased as the water table dropped. Increasing F_{CH_4} with a drop in the water table position from the soil surface has also been reported for subarctic fens in northern Quebec (Windsor et al., 1992) and Siberia (Heyer et al., 2002), tame pastureland in southeastern Manitoba (Tenuta et al., 2010), and riparian areas in a prairie pot-hole landscape in south-central Manitoba (Dunmola et al., 2010). It is suggested that water above a peat surface forms an aquatic environment whereby transport of CH_4 through diffusion and ebullition are less efficient than transport through air (Zona et al., 2009). Heyer et al. (2002) proposed that the low solubility of CH_4 causes bubble formation in near-surface soil overlain by water. As the water table lowers, release of hydrostatic pressure results in escape of bubbles through open soil pores connected to the atmosphere. We speculate that emission bursts of CH_4 were not observed at our fen during spring-melt partly as the result of the water table residing at or above the mean sedge-peat surface impeding the transport of CH_4 to the atmosphere.

An ice barrier impeded diffusion and ebullition of CH_4 further during the melt period of 2009 at our fen. Snow that had accumulated on top of the ice in winter had melted out quickly and left open water over an ice layer that extended down 10 to 30 cm to the peat surface. The ice thawed from the top downwards over the course of the melt period and despite $T_{soil5} \geq 0\,^{\circ}C$ allowing for soil microbial activity, CH_4 was trapped by this ice barrier and overlying water, slowing CH_4 release to the atmosphere. Hargreaves et al. (2001) described a similar occurrence of an ice barrier layer during spring melt at their permafrost-free aapa mire in Finland however they observed F_{CH_4} bursts which coincided with soil thawed > 40 cm and the occurrence of gases bubbling out from cracks in the ice barrier layer.

Across all springs, NEE_{MD} was not significantly correlated to F_{CH_4}. NEE_{MD} was respiration-dominated indicating that although new shoots from sedges were beginning to photosynthesize and provide some carbon in root exudates, the soil microbial communities were more effectively metabolising over-winter-stored carbon, respiring from hummocks exposed above the water table, and emitting CO_2 by diffusion through the water column from the aerobic peat-water interface. Methane was being produced in thawing anaerobic soils but in early spring the high water table inundated most of the fen. Methane could have been emitted through ebullition but we cannot be sure we captured these events during our campaigns. New sedge shoots were too small during spring melt to transfer much methane through their aerenchyma. Diffusion through the water column therefore dominated; a slow process due to methane's low solubility in water. Additionally, because the thaw layer of peat was shallow during melt, it is suggested that methane produced in the anaerobic layer was largely consumed as it moved upwards into the shallow aerobic peat-water interface. Across all falls, NEE_{MD} had a positive correlation with F_{CH_4}. At this time, water table was mostly below the peat surface, plants had senesced and soil microbial communities were metabolizing labile carbon of roots and above-ground plant biomass, emitting both CO_2 and CH_4 to the atmosphere at a decreasing rate as resources depleted and temperatures declined.

4.3 Cumulative annual CH_4 emissions

Cumulative annual CH_4 emissions for our fen ranged from 3.0 to 9.6 g CH_4 m^{-2} yr^{-1} between the study years of 2008 to 2011; we found the mean annual flux ±1 SE over the four years ranging from 6.6 ± 0.6 to 7.1 ± 1.1 g CH_4 m^{-2} yr^{-1} when comparing the three gap-filling techniques. Of the three gap-filling techniques, modelling the missing 30-min F_{CH_4} values using the linear T_{soil5} relationship with F_{CH_4} (for all shoulder + growing seasons) provided an underestimation of cumulative annual CH_4 emissions for 2008 and 2009 and an overestimation in 2010. The cap on F_{CH_4} at $T_{soil5} > 12\,^{\circ}C$ was likely the reason for the underestimated growing season flux values in 2008 and 2009. For 2010, this method overestimated F_{CH_4} in the growing season compared to measured values because the high water table overwhelmed the temperature relationship, and this is not taken into account within this gap-filling model. We suggest that the more accurate representation of the cumulative annual CH_4 emissions were obtained by gap-filling using linear interpolation between measured points.

BGD
10, 4539–4574, 2013

The cumulative annual CH_4 emission results calculated in this study are within range with fluxes measured from other northern peatland sites within the zone of continuous permafrost using the eddy covariance technique. Tagesson et al. (2012) estimated cumulative annual CH_4 emissions of 8.7 to 10 g CH_4 m^{-2} yr^{-1} for their patterned fen at Zackenberg, Greenland, Wille et al. (2008) estimated 3.2 g CH_4 m^{-2} yr^{-1} for a wet polygonal tundra at Lena River Delta, Siberia, and Hargreaves et al. (2001) estimated 5.5 g CH_4 m^{-2} yr^{-1}, modelled from data obtained during three field seasons at an aapa mire, Kaamanen, Finland. Larger cumulative annual CH_4 emissions were found in zones of discontinuous or no permafrost. Jackowicz-Korczynski et al. (2010) estimated 24.5 to 29.5 g CH_4 m^{-2} yr^{-1} from eddy covariance measurements at a palsa mire underlain by discontinuous permafrost at Stordalen, Sweden, whereas Rinne et al. (2008) reported 12.6 g CH_4 m^{-2} yr^{-1} from a boreal minerotrophic fen with no permafrost at Siikaneva, Finland. Hendriks et al. (2007) estimated 41 to 44 g CH_4 m^{-2} yr^{-1} from chamber measurements at a permafrost-free abandoned peat meadow at Horstermeer, Netherlands. Rouse et al. (1995) used dark vented 18-L chambers at our same fen site at Churchill, estimating an average daily F_{CH_4} of 22 and 62 mg CH_4 m^{-2} d^{-1} for specific times of year in 1989 and 1990 respectively. Our fluxes ranged from 25 to 92 mg CH_4 m^{-2} d^{-1} for that same time period (21 June to 11 September) showing good agreement.

5 Conclusions

Near-surface soil temperature and air temperature were the main controlling factors for F_{CH_4} from the subarctic fen in northern Manitoba explaining about 90 % of the variation. F_{CH_4} was essentially zero during frozen conditions. Emission bursts were not observed across all springs but two natural emission bursts were observed during fall of 2011. The seasonal pattern followed the temperature, and a temperature decrease coinciding with heavy rainfall inundating the fen during the growing season caused an immediate decrease in F_{CH_4} indicating that a high water table above the sedge-peat surface

BGD
10, 4539–4574, 2013

can overwhelm the temperature relationship. The temperature-response of F_{CH_4} was significantly greater in spring than fall, providing great insight into changing seasonal responses of F_{CH_4} to environmental drivers. Cumulative annual CH_4 emissions ranged from 3.0 to 9.6 g $CH_4\,m^{-2}\,yr^{-1}$ between the years 2008 and 2011, with mean annual CH_4 emissions ranging between 6.6 and 7.1 $CH_4\,m^{-2}\,yr^{-1}$ using different gap-filling techniques. Our annual CH_4 emissions are within the range of measurements at other northern fen environments underlain by continuous permafrost.

Acknowledgements. We thank staff, researchers and volunteers of the Churchill Northern Studies Centre, C. Basler, K. Davoli, J. Dunn, L. Fishback, R. Hermans, K. Jansen, S. Kuleza, C. Paddock, and J. Rutter for field support, Z. Nesic (software), J. O. Rapai and K. Swystun for technical support. Funding was provided by the Natural Sciences and Engineering Research Council of Canada (NSERC) Discovery Program, the Canada Foundation for Innovation, the Canada Research Chair Program in Applied Soil Ecology and ArcticNet Network of Centres of Excellence of Canada. K. H. was supported by a NSERC Postgraduate Scholarship, the W. Garfield Weston Award for Northern Research, the Northern Scientific Training Program, the Environment Canada Science Horizons Program and the Churchill Northern Studies Centre Northern Research Fund.

References

Baer, D. S., Paul, J. B., Gupta, M., and O'Keefe, A.: Sensitive absorption measurements in the near-infrared region using off-axis integrated-cavity-output spectroscopy, Appl. Phys. B-Laser O., 75, 261–265, 2002.

Baldocchi, D., Detto, M., Sonnentag, O., Verfaillie, J., The, Y. A., Silver, W., and Kelly, N. M.: The challenges of measuring methane fluxes and concentrations over peatland pasture, Agric. Forest Meteorol., 153, 177–187, doi:10.1016/j.agrformet.2011.04.013, 2011.

Brown, R. J. E.: Permafrost in Canada; its Influence on Northern Development, Canadian Building Series 4, University of Toronto Press, Toronto, 1970.

Burba, G. G., McDermitt, D. K., Grelle, A., Anderson, D. J. and Xu, L.: Addressing the influence of instrument surface heat exchange on the measurements of CO_2 from open-path gas analyzers, Glob. Change Biol., 14, 1854–1876, 2008.

Detto, M., Verfaillie, J., Anderson, F., Xu, L., and Baldocchi, D.: Comparing laser-based open- and closed-path gas analyzers to measure methane fluxes using the eddy covariance method, Agric. Forest Meteorol., 151, 1312–1324, 2011.
Duguay, C. R., Pultz, T. J., Lafleur, P. M., and Drai, D.: RADARSAT backscatter characteristics of ice growing on shallow sub-Arctic lakes, Churchill, Manitoba, Canada, Hydrol. Process., 16, 1631–1644, 2002.
Dunmola, A. S., Tenuta, M., Moulin, A. P., Yapa, P., and Lobb, D. A.: Pattern of greenhouse gas emission from a Prairie Pothole agricultural landscape in Manitoba, Canada, Can. J. Soil Sci., 90, 243–256, 2010.
Edwards, K. A., McCullough, J., Kershaw, G. P., and Jeffries, R. L.: Soil microbial and nutrient dynamics in a wet Arctic sedge meadow in late winter and early spring, Soil Biol. Biochem., 38, 2843–2851, 2006.
Environment Canada: National climate data and information archive, http://www.climate.weatheroffice.gc.ca, 2012.
Forster, P., Ramaswamy, V., Artaxo, P., Berntsen, T., Betts, R., Fahey, D. W., Haywood, J., Lean, J., Lowe, D. C., Myhre, G., Nganga, J., Prinn, R., Raga, G., Schulz, M., and Van Dorland, R.: Changes in atmospheric constituents and in radiative forcing, in: Climate Change 2007: The Physical Science Basis. Contribution of Working Group I to the Fourth Assessment Report of the Intergovernmental Panel on Climate Change, edited by: Solomon, S., Qin, D., Manning, M., Chen, Z., Marquis, M., Averyt, K. B., Tignor, M., and Miller, H. L., Cambridge University Press, Cambridge, UK and New York, USA, 2007.
Grondahl, L., Friborg, T., Christensen, T. R., Ekberg, A., Elberling, B., Illeris, L., Nordstrom, C., Rennermalm, A., Sigsgaard, C., and Sogaard, H.: Spatial and inter-annual variability of trace gas fluxes in a heterogeneous high-Arctic landscape, Adv. Ecol. Res., 40, 473–498, 2008.
Hargreaves, K. J., Fowler, D., Pitcairn, C. E. R., and Aurela, M.: Annual methane emission from Finnish mires estimated from eddy covariance campaign measurements, Theor. Appl. Climatol., 70, 203–213, 2001.
Hendriks, D. M. D., Dolman, A. J., van der Molen, M. K., and van Huissteden, J.: A compact and stable eddy covariance set-up for methane measurements using off-axis integrated cavity output spectroscopy, Atmos. Chem. Phys., 8, 431–443, doi:10.5194/acp-8-431-2008, 2008.
Hendriks, D. M. D., van Huissteden, J., and Dolman, A. J.: Multi-technique assessment of spatial and temporal variability of methane fluxes in a peat meadow, Agric. Forest Meteorol., 150, 757–774, 2010.

Heyer, J., Berger, U., Kuzin, I. L., and Yakovlev, O. N.: Methane emissions from different ecosystem structures of the subarctic tundra in Western Siberia during midsummer and during the thawing period, Tellus, 54B, 231–249, 2002.
Jackowicz-Korczynski, M., Christensen, T. R., Backstrand, K., Crill, P., Friborg, T., Mastepanov, M., and Strom, L.: Annual cycle of methane emission from a subarctic peatland, J. Geophys. Res. Biogeo., 115(G2), G02009, doi:10.1029/2008JG000913, 2010.
Kleinbaum, D. G. and Kupper, L. L.: Applied Regression Analysis and Other Multivariable Methods. Duxberry Press, North Scituate, MA, 1978.
Long, K. D., Flanagan, L. B., and Cai, T.: Diurnal and seasonal variation in methane emissions in a northern Canadian peatland measured by eddy covariance, Glob. Change Biol., 16, 2420–2435, 2009.
Los Gatos Research: Methane Analyzers: Fast–Low Power–High Precision, http://www.lgrinc.com/documents/Methane-Analyzers-web.pdf, 2009.
Mastepanov, M., Sigsgaard, C., Dlugokencky, E. J., Houweling, S., Strom, L., Tamstorf, M. P., and Christensen, T. R.: Large tundra methane burst during onset of freezing, Nature, 456, 628–630, 2008.
McGuire, A. D., Anderson, L. G., Christensen, T. R., Dallimore, S., Guo, L., Hayes, D. J., Heimann, M., Lorenson, T. D., Macdonald, R. W., and Roulet, N.: Sensitivity of the carbon cycle in the Arctic to climate change, Ecol. Monogr., 79, 523–555, 2009.
National Wetlands Working Group: The Canadian Wetland Classification System: Second Edition, Wetland Research Centre, University of Waterloo, Ontario, 1997.
Pickett-Heaps, C. A., Jacob, D. J., Wecht, K. J., Kort, E. A., Wofsy, S. C., Diskin, G. S., Worthy, D. E. J., Kaplan, J. O., Bey, I., and Drevet, J.: Magnitude and seasonality of wetland methane emissions from the Hudson Bay Lowlands (Canada), Atmos. Chem. Phys., 11, 3773–3779, doi:10.5194/acp-11-3773-2011, 2011.
Raddatz, R. L., Papakyriakou, T. N., Swystun, K. A., and Tenuta, M.: Evapotranspiration from a wetland tundra sedge fen: surface resistance of peat for land-surface schemes, Agric. Forest Meteorol., 149, 851–861, 2009.
Rinne, J., Riutta, T., Pihlatie, M., Aurela, M., Haapanala, S., Tuovinen, J. P., Tuittila, E. S., and Vesala, T.: Annual cycle of methane emission from a boreal fen measured by the eddy covariance technique, Tellus, 59B, 449–457, 2007.
Rouse, W. R., Holland, S., and Moore, T. R.: Variability in methane emissions from wetlands at northern treeline near Churchill, Manitoba, Arctic Alpine Res., 27, 146–156, 1995.

Rouse, W. R., Bello, R. L., D'Souza, A., Griffis, T. J. and Lafleur, P. M.: The annual carbon budget for fen and forest in a wetland at Arctic treeline, Arctic, 55, 229–237, 2002.
Schimel, J. P.: Plant transport and methane production as controls on methane flux from Arctic wet meadow, Biogeochemistry, 28, 183–200, 1995.
Shindell, D. T., Galuvegi, G., Koch, D. M., Schmidt, G. A., Unger, N., and Bauer, S. E.: Improved attribution of climate forcing to emissions. Science, 326, 716–718, 2009.
Tagesson, T., Molder, M., Mastepanov, M., Sigsgaard, C., Tamstorf, M. P., Lund, M., Falk, J. M., Lindroth, A., Christensen, T. R., and Strom, L.: Land-atmosphere exchange of methane from soil thawing to soil freezing in a high-Arctic wet tundra ecosystem, Glob. Change Biol., 18, 1928–1940, doi:10.1111/j.1365-2486.2012.02647.x, 2012.
Tanner, C. B. and Thurtell, G. W.: Sensible Heat Flux Measurements with a Yaw Sphere and Thermometer: Anemoclinometer Measurements of Reynolds Stress and Heat Transport in the Atmospheric Surface Layer. TR Ecom 66-G22-F, Dept. Soil Science, Univ. Wisconsin, Madison, WI, 1969.
Tarnocai, C., Canadell, J. G., Schuur, E. A. G., Kuhry, P., Mazhitova, G., and Zimov, S.: Soil organic carbon pools in the northern circumpolar permafrost region, Glob. Biogeochem. Cy., 23, GB2023, doi:10.1029/2008GB003327, 2009.
Tenuta. M., Mkhabela, M., Tremorin, D., Coppi, L., Phipps, G., Flaten, D., and Ominski, K.: Nitrous oxide and methane emission from a coarse-textured grassland soil receiving hog slurry, Agr. Ecosyst. Environ., 138, 35–43, 2010.
Tokida, T., Mizoguchi, M., Miyazaki, T., Kagemoto, A., Nagata, O., and Hatano, R.: Episodic release of methane bubbles from peatland during spring thaw, Chemosphere, 70, 165–171, 2007.
Turetsky, M. R., Treat, C. C., Waldrop, M. P., Waddington, J. M., Harden, J. W., and McGuire, A. D.: Short-term response of methane fluxes and methanogen activity to water table and soil warming manipulations in an Alaskan peatland, J. Geophys. Res.-Biogeo., 113, G00A10, doi:10.1029/2007JG000496, 2008.
Updegraff, K., Bridgham, S. D., Pastor, J., Weishampel, P., and Harth, C.: Response of CO_2 and CH_4 emissions from peatlands to warming and water table manipulations, Ecol. Appl., 11, 311–326, 2001.
Verville, J. H., Hobbie, S. E., Chapin, F. S., and Hooper, D. U.: Response of tundra CH_4 and CO_2 flux to manipulation of temperature and vegetation, Biogeochemistry, 41, 215–235, 1998.

BGD
10, 4539–4574, 2013

Seasonal dynamics of methane emissions from a subarctic fen

K. L. Hanis et al.

Webb, E. K., Pearman, G., and Leuning, R.: Correction of flux measurements for density effects due to heat and water vapour transfer, Quart. J. Roy. Meteorol. Soc., 106, 85–100, 1980.
Wille, C., Kutzbach, L., Sachs, T., Wagner, D., and Pfeiffer, E. M.: Methane emission from Siberian Arctic polygonal tundra: eddy covariance measurements and modeling, Glob. Change Biol., 14, 1395–1408, 2008.
Windsor, J., Moore, T. R., and Roulet, N. T.: Episodic fluxes of methane from subarctic fens, Can. J. Soil Sci., 72, 441–452, 1992.
Zona, D., Oechel, W. C., Kochendorfer, J., Paw U, K. T., Salyuk, A. N., Olivas, P. C., Oberbauer, S. F., and Lipson, D. A.: Methane fluxes during the initiation of a large-scale water table manipulation experiment in the Alaskan Arctic tundra, Glob. Biogeochem. Cy., 23, GB2013, doi:10.1029/2009GB003487, 2009.

BGD
10, 4539–4574, 2013

Table 1. Summary table of monthly mean air temperature (T_{air}) and total precipitation compared to the 1971–2000 Climate Normals for Churchill, Manitoba obtained from Environment Canada. – = no data available; ∼= 312 mm precipitation for June to November for use in 2009 and 2011 comparisons.

	May	Jun	Jul	Aug	Sep	Oct	Nov	Season Total
Mean T_{air} (°C)								
2008	−0.5	7.3	12.5	13.8	5.2	1.5	−9.3	4.4
2009	−6.9	3.3	8.6	10.5	8.9	−0.3	−7.3	2.4
2010	−1.1	7.7	14.0	11.1	6.8	1.7	−8.1	4.6
2011	−2.2	7.7	14.2	13.0	10.3	1.7	−9.3	5.1
Normal	*−0.7*	*6.6*	*12.0*	*11.7*	*5.6*	*−1.7*	*−12.6*	*3.0*
Precipitation (mm)								
2008	21	43.0	20.1	81.5	53.0	50.4	7.0	276.0
2009	–	45.9	91.5	21.6	65.3	25.4	14.4	264.1
2010	40.9	12.5	71.9	181.4	54.2	27.2	6.9	395.0
2011	–	42.9	59.8	80.2	24.2	102.0	12.8	321.9
Normal	*31.9*	*44.3*	*56.0*	*68.3*	*63.4*	*46.9*	*33.1*	*343.9* ∼

BGD
10, 4539–4574, 2013

Table 2. Pearson product moment correlation analysis for 30 min averaged F_{CH_4} data and environmental variables. Correlations are shown for spring of 2009 (DOY 150–190), all springs (DOY 150–190, 2008–2011), fall of 2011 (DOY 260–320), all falls (DOY 260–320, 2008–2011) and all shoulder + growing seasons (DOY 150–320, 2008–2011) data. NS = $P > 0.0001$ (statistically insignificant) and – = data not available.

		T_{air}	T_{soil5}	T_{hol10}	T_{hol20}	T_{hol50}	T_{sed10}	T_{sed20}	T_{sed50}	NEE_{MD}	WT	PAR
Spring	R	0.68	0.84	0.87	0.88	0.85	0.89	–	0.70	0.53	−0.66	−0.27
2009	N	273	273	273	273	273	273	0	273	59	173	273
All	R	0.72	0.85	0.85	0.72	0.84	0.81	NS	0.74	NS	−0.70	NS
Springs	N	311	311	311	311	311	311	38	311	77	203	311
Fall	R	0.74	0.75	0.67	0.66	0.63	0.74	0.68	NS	NS	NS	0.55
2011	N	86	86	86	86	86	86	86	80	11	46	86
All	R	0.77	0.86	0.82	0.83	0.82	0.83	0.82	0.76	0.57	NS	0.61
Falls	N	333	312	312	312	312	312	309	306	61	72	333
All Shoulder	R	0.57	0.52	0.30	NS	−0.24	0.54	0.41	−0.26	NS	−0.15	0.30
+ Growing	N	1515	1455	1465	1465	1404	1431	1137	1459	449	1021	1515

Table 3. Cumulative annual CH_4 emissions for all days when daily mean air temperature $\geq 0\,^{\circ}C$ gap-filled by (1) using linear interpolation to gap-fill missing days between measured F_{CH_4}($\Sigma F_{CH_4-GF_1}$), (2) using linear interpolation to fill 30-min gaps between measured F_{CH_4}($\Sigma F_{CH_4-GF_2}$), and (3) modelling the missing 30-min F_{CH_4} values using the T_{soil5} linear regression relationship with F_{CH_4} (for all shoulder + growing seasons) up to 12 °C and above this temperature, the daily flux was assumed constant at 47 nmol $CH_4\,m^{-2}\,s^{-1}$ ($\Sigma F_{CH_4-GF_3}$). Mean annual CH_4 emissions ±1 SE for the study years 2008–2011 also shown.

		2008	2009	2010	2011	Mean ±1 SE
$\Sigma F_{CH_4-GF_1}$	($g\,CH_4\,m^{-2}\,yr^{-1}$)	9.5	6.4	4.3	8.0	7.1 ± 1.1
$\Sigma F_{CH_4-GF_2}$	($g\,CH_4\,m^{-2}\,yr^{-1}$)	9.6	7.6	3.0	8.0	7.0 ± 1.4
$\Sigma F_{CH_4-GF_3}$	($g\,CH_4\,m^{-2}\,yr^{-1}$)	6.6	4.8	7.2	7.6	6.5 ± 0.6

BGD
10, 4539–4574, 2013

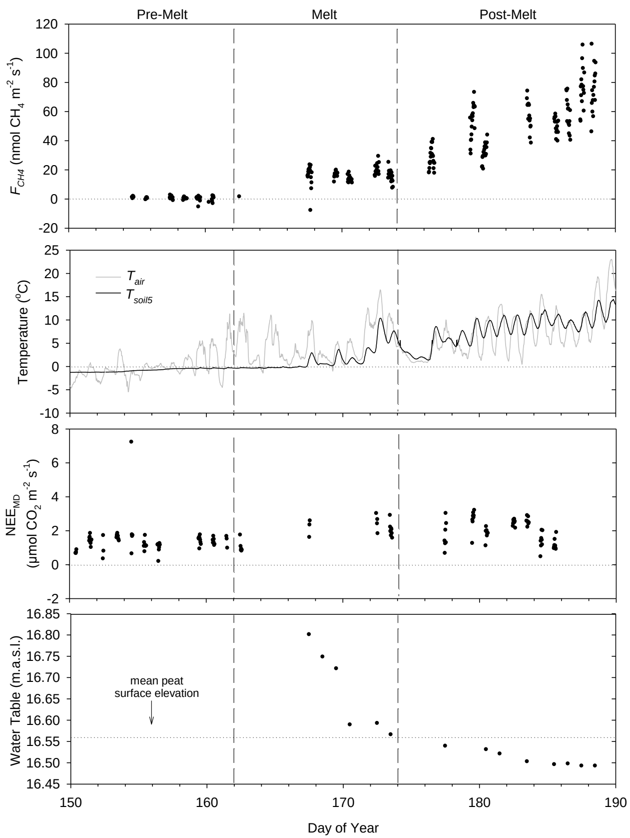

Fig. 1. Spring of 2009 30-min CH_4 flux (F_{CH_4}), air temperature (T_{air}), 5 cm soil temperature (T_{soil5}), midday net CO_2 flux (NEE_{MD}) and water table height for the fen from 30 May to 9 July 2009 (DOY 150 to 190).

BGD
10, 4539–4574, 2013

Seasonal dynamics of methane emissions from a subarctic fen

K. L. Hanis et al.

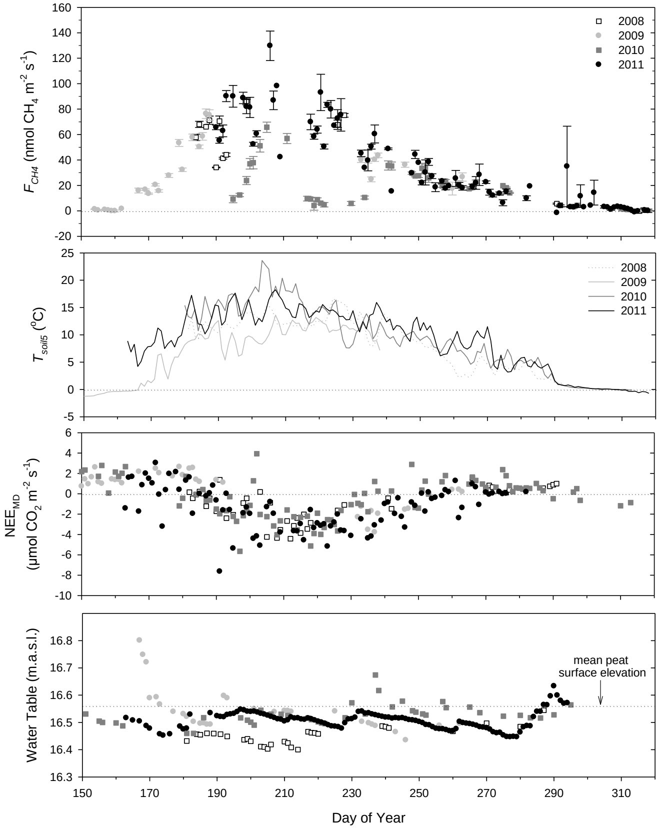

Fig. 2. Mean daily CH_4 flux (F_{CH_4}) (no gap-filling) for 30 min averaged campaign periods (n = 1 to 48) ±1 SE shown, and mean daily 5 cm soil temperature (T_{soil5}), midday net CO_2 flux (NEE_{MD}) and water table height for all shoulder + growing seasons (DOY 150–320, 2008–2011).

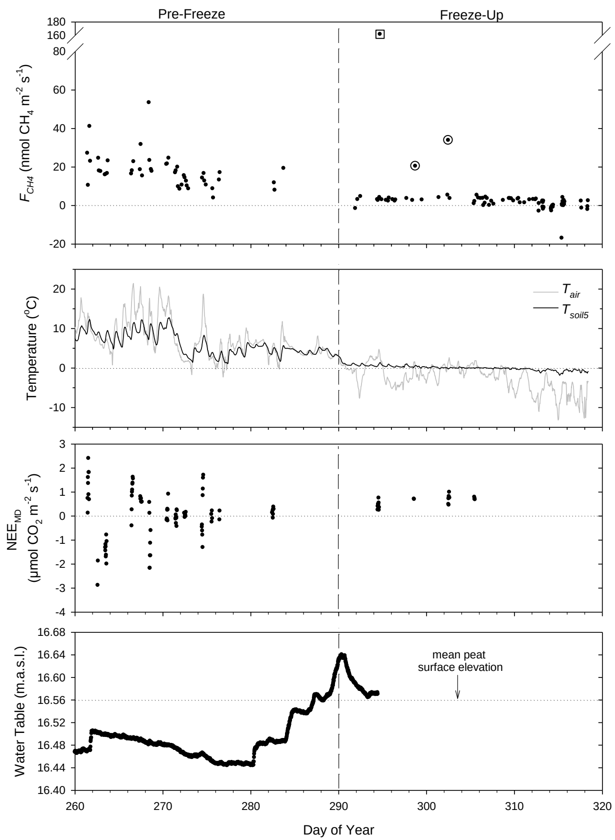

Fig. 3. Fall of 2011 30-min CH_4 flux (F_{CH_4}), air temperature (T_{air}), 5 cm soil temperature (T_{soil5}), midday net CO_2 flux (NEE_{MD}) and water table height for the fen from 17 September to 16 November 2011 (DOY 260–320). Open square indicates an anthropogenic emission burst, while open circles indicate natural emission bursts.

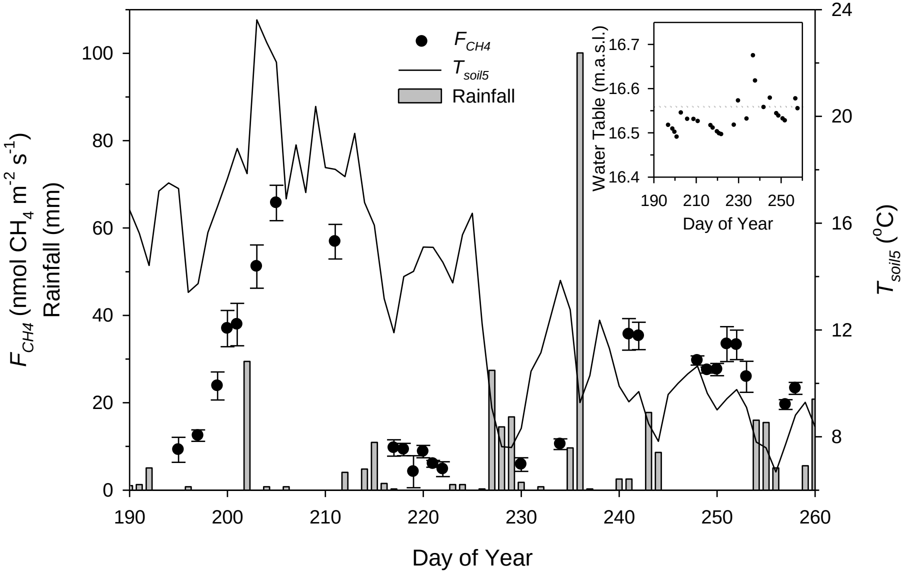

Fig. 4. Growing season mean daily CH_4 flux (F_{CH_4}) (no gap-filling) ($n = 3$ to 42) ±1 SE shown, mean daily 5 cm soil temperature (T_{soil5}) and total daily rainfall for the fen from 9 July to 17 September 2010 (DOY 190–260). Inset Figure: Mean daily water table height for the fen from 9 July to 17 September 2010 (DOY 190–260). Dotted line indicates the mean peat surface elevation.

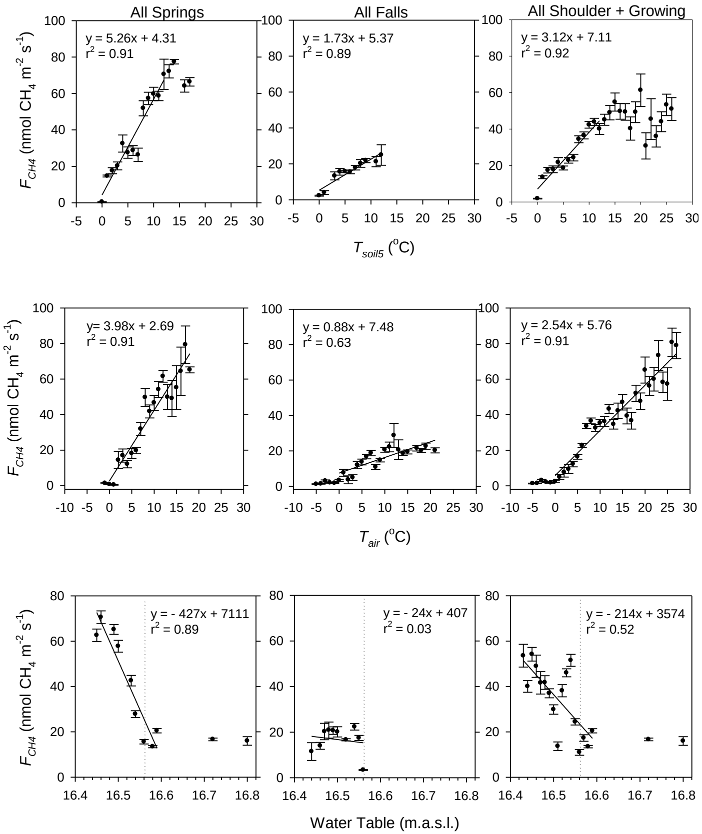

Fig. 5. Bin-averaged (1 °C) 30-min CH_4 flux (F_{CH_4}) ±1 SE in response to soil temperature at 5 cm (T_{soil5}) and air temperature (T_{air}) shown for all springs (DOY 150 to 190, 2008–2011), all falls (DOY 260 to 320, 2008–2011) and all shoulder + growing seasons (DOY 150–320, 2008–2011). Bin-averaged (1 cm water table height) 30-min CH_4 flux (F_{CH_4}) ±1 SE in response to water table is shown for the same periods. Dotted line indicates the mean peat surface elevation.